

## Giant Enhancement of Optical Second Harmonic Generation in Hollow-Core Fiber Integrated with GaSe Nanoflakes

Xiaoyu Wang<sup>1,2,†</sup>, Yang Cheng<sup>1,†</sup>, Guodong Xue<sup>1</sup>, Ziqi Zhou<sup>1</sup>, Mengze Zhao<sup>1</sup>, Chaojie Ma<sup>1</sup>, Jin Xie<sup>1,2</sup>, Guangjie Yao<sup>1,2</sup>, Hao Hong<sup>1</sup>, Xu Zhou<sup>4,\*</sup>, Kaihui Liu<sup>1,\*</sup>, Zhongfan Liu<sup>2,3,\*</sup>

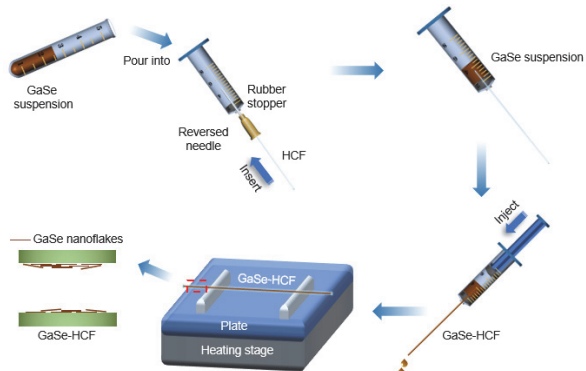
<sup>1</sup> State Key Laboratory for Mesoscopic Physics, Frontiers Science Center for Nano-optoelectronics, School of Physics, Peking University, Beijing 100871, China.

<sup>2</sup> Beijing Graphene Institute (BGI), Beijing 100095, China.

<sup>3</sup> Center for Nanochemistry, College of Chemistry and Molecular Engineering, Peking University, Beijing 100871, China.

<sup>4</sup> Guangdong Provincial Key Laboratory of Quantum Engineering and Quantum Materials, School of Physics and Telecommunication Engineering, South China Normal University, Guangzhou 510006, China.

**Abstract:** All-fiber functional devices are superior to conventional optical crystals for next-generation integrated optics owing to their natural compatibility with optical fiber systems. Nonlinear optical fiber devices play an important role in frequency conversion and optical parametric amplification. However, optical fibers are unsuitable for all-optical systems owing to the intrinsic properties of pure quartz. Optical second harmonic generation (SHG), which is significant in practical optical applications, is theoretically forbidden in traditional centrosymmetric non-crystalline fused silica fibers. Consequently, generating giant second-order optical processes in optical fibers remains challenging. Many studies have attempted to artificially break the centrosymmetry of fused silica fibers using various poling techniques, such as thermal or electric field poling, which can enhance the second-order nonlinear optical susceptibility. However, these methods require difficult and complicated fabrication processes, and the corresponding hybrid optical fibers exhibit an inefficient harmonic generation process, which greatly increases the cost and limits the development of all-fiber nonlinear functionalization. Therefore, there is an urgent need for new fabrication methods and technical means for functionalizing optical fiber devices that can improve the second-order nonlinear effect while remaining simple and practical. Herein, we propose an improved solution-filling method that can effectively deposit highly nonlinear GaSe nanoflakes directly on the inner walls of hollow-core fibers (HCF) with a length of up to half a meter. In addition, the as-fabricated hollow-core fiber integrated with GaSe nanoflakes (GaSe-HCF) is used to demonstrate that the second-order nonlinear effect of the optical fiber is enhanced by the ultrahigh nonlinear effect of the GaSe materials. Compared to previously reported MoS<sub>2</sub>-embedded hollow-core fibers (MoS<sub>2</sub>-HCF) and conventional optical fibers, the SHG of the GaSe-HCF is three and two orders of magnitude stronger than that of bare HCF and MoS<sub>2</sub>-HCF, respectively. A GaSe-HCF with a length of up to half a meter was successfully prepared using the new filling method and exhibited good expansibility. The pressure process was exploited by adding a short length



Received: December 17, 2022; Revised: January 19, 2023; Accepted: January 20, 2023; Published online: February 7, 2023.

†These authors contributed equally to this work.

\*Corresponding authors. Emails: xuzhou2020@m.scnu.edu.cn (X.Z.); khliu@pku.edu.cn (K.L.); zfliu@pku.edu.cn (Z.L.).

The project was supported by the National Key R&D Program of China (2021YFA1400201, 2021YFB3200303, 2021YFA1400502, 2022YFA1403504), the National Natural Science Foundation of China (52021006, 52172035, 92163206, 52025023, 12104018), the Strategic Priority Research Program of Chinese Academy of Sciences (XDB33000000), the China Postdoctoral Science Foundation (2021T140022), the Guangzhou Basic and Applied Basic Research Projects (202201010395).

国家重点研发计划(2021YFA1400201, 2021YFB3200303, 2021YFA1400502, 2022YFA1403504), 国家自然科学基金(52021006, 52172035, 92163206, 52025023, 12104018), 中国科学院战略重点研究计划(XDB33000000), 中国博士后科学基金(2021T140022), 广州市基础与应用基础研究(202201010395)资助项目

of air column to effectively fill the HCF with the highly nonlinear GaSe suspension, and expand the applicability of this method. Our results will provide a novel and highly efficient strategy to manufacture nonlinear optical fibers integrated with other nanomaterials and can be used to fabricate new all-fiber devices with strongly enhanced second-order nonlinear optical processes, thus broadening nonlinear optics and optoelectronics applications.

**Key Words:** Hollow-core fiber; Gallium selenide; SHG; Optical frequency converter; Solution filling method; Nanomaterials

## 基于硒化镓纳米片填充的空芯光纤超高二次谐波增强

王晓愚<sup>1,2,†</sup>, 程阳<sup>1,†</sup>, 薛国栋<sup>1</sup>, 周子琦<sup>1</sup>, 赵孟泽<sup>1</sup>, 马超杰<sup>1</sup>, 谢瑾<sup>1,2</sup>, 姚光杰<sup>1,2</sup>, 洪浩<sup>1</sup>, 周旭<sup>4,\*</sup>, 刘开辉<sup>1,\*</sup>, 刘忠范<sup>2,3,\*</sup>

<sup>1</sup>北京大学物理学院, 纳米光电子前沿科学中心, 介观物理国家重点实验室, 北京 100871

<sup>2</sup>北京石墨烯研究院(BGI), 北京 100095

<sup>3</sup>北京大学化学与分子工程学院, 纳米化学中心, 北京 100871

<sup>4</sup>华南师范大学物理与通信工程学院, 广东省量子工程与量子材料重点实验室, 广州 510006

**摘要:** 与传统的光学晶体相比, 全光纤功能器件由于和光纤系统的天然兼容性, 被认为是下一代集成光学的重要研究方向, 吸引了人们的广泛关注。然而, 由于二氧化硅固有的中心反演对称性质, 光纤中的二阶非线性光学过程仍有待探索, 这在可调谐超快激光、全光信号处理、成像和光通信等商业全光纤非线性光学应用中具有重要意义。因此, 我们提出了一种新的溶液填充方法, 可有效地将具有高非线性的硒化镓纳米片直接沉积在长度达半米的空芯光纤(HCF)的内孔壁上。此外, 采用制备的硒化镓纳米片-空芯光纤(GaSe-HCF)作为光频率转换器, 其二次谐波(SHG)比嵌入MoS<sub>2</sub>的HCF和普通HCF分别提高了2个数量级和3个数量级。我们的研究成果将拓展其它非线性材料在全光纤高端非线性光学和光电子学中的应用, 并提供新的制备思路。

**关键词:** 空芯光纤; 硒化镓; 光学二次谐波; 光频率转换器; 溶液填充法; 纳米材料

**中图分类号:** O645

### 1 Introduction

Optical fibers have been the foundation of modern communications, and they are constantly developed into many types of optical fiber devices for constructing all-fiber optical systems, due to the advantages of high communication capacity, high integration, and small volume. High nonlinear optical fibers and based-fiber devices play an important role in frequency conversion and optical parametric amplification. However, as an important and efficient nonlinear process, the second-order nonlinear process does not occur in conventional optical fiber because of the intrinsic inversion symmetry of fused silica. SHG in optical fiber has been intensively studied for more than 30 years since it was discovered in doped-silica fibers in the early 1980s<sup>1</sup>. Great efforts have been devoted to introducing the periodic structure in fiber to meet the quasi-phase matching conditions of the SHG, including periodic poling by thermal process<sup>2–4</sup>, external electric field<sup>5–8</sup>, or optical field<sup>9–11</sup> on silica optical fibers. However, those methods need to meet some extremely confined conditions like over kilovolts voltage, high temperatures over 200 °C, or high-power femtosecond lasers, thus inevitably introducing complex fabrication processes.

Integrating other materials with optical fiber to enhance SHG is another approved effective way, such as two-dimensional transition metal dichalcogenides with high second-order optical nonlinear susceptibilities<sup>12,13</sup>. The integration of few-layer nonlinear nanomaterials and optical fiber can effectively enhance the SHG conversion efficiency in the optical fiber by increasing the interaction length. Recently, Liu *et al.*<sup>13</sup> successfully fabricated optical fibers with ultrahigh nonlinearity by embedding two-dimensional MoS<sub>2</sub> crystals into the holes of a photonic crystal fiber or an HCF by a chemical vapor deposition method, which opens a new horizon for all-fiber nonlinear optics and optoelectronics applications. In addition, Zhao *et al.*<sup>14</sup> focused on integrating high-nonlinearity few-layer materials with different structural fibers by using a dip-coating technique to enhance second-order nonlinear processes under nonresonant excitation conditions. However, the existing fabrication methods still have some issues, such as inefficient nonlinear conversion efficiencies, complicated fabrication processes, and batch manufacturing difficulties. Thus, it is essential to develop more efficient routes to integrate micro-nano scale materials and optical fibers to realize commercial

applications of high-nonlinearity and multi-functional nanomaterials in all-fiber systems.

Here, we report a novel syringe-filling method for the convenient and scalable fabrication of GaSe-HCF with a length of up to half a meter. With its simple and unique structural characteristics of hollow core, the HCF has been a novel platform for all-fiber optical devices, including low-loss optical waveguides<sup>15–17</sup>, fiber sensors<sup>18–22</sup>, mode-locked fiber lasers<sup>23–25</sup>, optical modulators<sup>26–31</sup>, and laser frequency converters<sup>32–37</sup>. The corresponding bulk GaSe is a well-known nonlinear crystal with second-order optical nonlinear coefficient 2 orders of magnitude larger than that of the widely used LiNbO<sub>3</sub> crystal<sup>38,39</sup>, and two-dimensional monolayer GaSe shows much stronger SHG intensity than other two-dimensional atomic crystals even under nonresonant condition<sup>12</sup>. Therefore, taking advantages of both the large second-order optical nonlinear coefficients of GaSe and the strong light-material interactions in HCFs, we report that the as-grown GaSe-HCF exhibits about two orders enhanced SHG intensity compared to high-nonlinearity MoS<sub>2</sub>-HCF consistent with the previous reports<sup>13</sup>. Our results propose a highly efficient fabrication strategy for the tight integration of various functional nanomaterials and porous fibers. The greatly enhanced SHG in GaSe-HCF suggests an exciting all-fiber device in nonlinear optics and optoelectronics applications.

## 2 Methods

### 2.1 Deposition of GaSe nanoflakes into HCFs

GaSe sources (99.999%, SixCarbon Technology Shenzhen, China) were grounded into nanoflakes with a diameter smaller than that of the inner hole of the HCF by using a mortar. For effectively and evenly filling the GaSe materials into the fiber, GaSe nanoflakes were dispersed in a GaSe-alcohol mixture and subjected to ultrasonic treatment for 10 min. Subsequently, a pipette was used to drop the mixed suspension into the barrel of the syringe, then the GaSe suspension can be successfully pre-filled into the HCF with the pressure of the air column produced by inserting the plunger into the barrel. Next, the pre-filled optical fiber was placed on a quartz plate which was loaded onto a heating stage. After that, the two ends of HCF were supported with PDMS pads and baked for 180 min at 80 °C for drying and deposition.

### 2.2 Characterization of GaSe-HCFs

Optical images were taken with an Olympus BX51M microscope by focusing on the holes in the fiber walls. Raman and *in situ* SHG spectra were collected with a homemade optical system excited using a 514 nm laser with a power of ~0.3 mW and a 1064 nm laser with a power of ~1 mW, respectively. A scanning electron microscope (Thermo Fisher, Quattro S, Thermo Fisher Scientific, USA) was used to characterize the morphology of the GaSe-HCF.

### 2.3 SHG measurements

Two systems were alternatively used in our harmonic generation measurement. The SHG spectra of GaSe-HCF,

MoS<sub>2</sub>-HCF, and bare HCF were measured with a commercial laser (Rainbow 1064 OEM, NPI Lasers, China). In addition, pump fluence-dependent SHG was excited using a Coherent Vitara-T oscillator and an optical parametric amplifier 9850 laser system (~100 fs, 250 kHz, 1200–1600 nm). The excitation laser was focused using a Nikon objective ( $\times 4$ , NA = 0.1). After filtering out the excitation laser, the SHG signal was recorded using a Princeton SP2500 spectrometer equipped with a nitrogen-cooled silicon charge couple device camera *via* a transition system.

## 3 Results and discussion

In our design, commercial few-layer GaSe nanoflakes with thicknesses of several nanometers up to ~2 μm were deposited onto the inner hole walls of an HCF (the hollow core diameter of ~50 μm and wall thickness of ~50 μm) by the novel syringe-filling method (Fig. 1). Compared with a capillary filling method based on the capillary effect<sup>13</sup>, the syringe-filling method is more efficient in directly injecting the solution into the HCF, especially for the solid-liquid mixed suspension. In the process, the problem of liquid leakage resulted from the mismatch between the fiber and the shaft of the needle (a bare HCF with a cladding of ~150 μm in diameter and needle hole of ~300 μm in diameter) is perfectly solved (Fig. 1), in which the extra glue in the gap and consequent secondary pollution are avoided. The sealing property provides a high enough pressure inside the syringe to effectively fill the solid-liquid mixed suspension into the HCF. The detailed procedures are as follows. (1) The end of the needle shaft is put into the rubber stopper, and one end of the HCF is inserted through the needle subsequently (Fig. 1a). (2) After that, a pipette is used to drop the suspension into the barrel

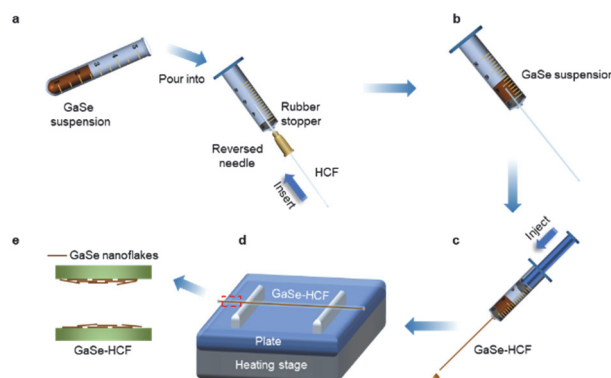


Fig. 1 The schematic of novel syringe-filling method.

The syringe structure is reconstructed by adding a rubber stopper at the front of the syringe and putting the end of the shaft of the needle into the rubber stopper, finally inserting the end of HCF through the needle. Subsequently, a pipette is used to drop the suspension into the barrel of the syringe, and the GaSe suspension can be successfully pre-filled into the HCF with the pressure of the air column between the plunger and the suspension by inserting the plunger into the barrel. Next, the pre-filled optical fiber is pulled out from the rubber stopper and placed on a quartz plate loaded onto a heating stage. After that, the two ends of HCF are supported with PDMS pads and baked for 180 min at 80 °C for drying and deposition. Eventually, the GaSe-HCF can be obtained.

of the syringe (Fig. 1b). (3) Then the GaSe suspension is successfully pre-filled into the HCF with the pressure of the air column produced by inserting the plunger into the barrel (Fig. 1c). (4) Next, the pre-filled optical fiber is pulled out from the rubber stopper and placed on a quartz plate loaded onto a heating stage. (5) In addition, both ends of HCF are supported with PDMS pads and baked for 180 min at 80 °C for drying and deposition (Fig. 1d). Eventually, the GaSe-HCF can be obtained (Fig. 1e). (6) In order to make GaSe coated into the HCF adequately, multiple deposition procedures are adopted to achieve a full-filled GaSe-HCF.

The successful filling of high-quality GaSe nanoflakes into the HCF is confirmed by *in situ* comprehensive characterizations (Fig. 2). The optical contrast of GaSe-HCF and bare HCF indicates the obvious difference that the yellow color in the fiber core region of GaSe-HCF is deeper than that in bare HCF, showing its full coverage of GaSe film on the fiber hole wall (Fig. 2a,b). Furthermore, to acquire direct evidence, we characterized the cross-sectional morphology of GaSe-HCF using a scanning electron microscope (SEM). As shown in the additional SEM images at different magnifications, we observed that the few-layer GaSe flakes are tightly attached to the hole walls and the thicknesses of the GaSe nanoflakes are in the range of several nanometers to 2 μm according to the SEM image (Fig. 2c). A typical Raman spectrum of GaSe flakes consisting of three characteristic peaks is depicted in Fig. 2d including the  $A_{1g}^1$  mode ( $\sim 132 \text{ cm}^{-1}$ ),  $E_{2g}^1$  mode ( $\sim 212 \text{ cm}^{-1}$ ), and  $A_{1g}^2$  mode ( $\sim 308 \text{ cm}^{-1}$ ), which is consistent with the previous report for GaSe flakes<sup>12,40–42</sup>. Among these modes,  $A_{1g}^1$  and  $A_{1g}^2$  modes correspond to the out-of-plane vibrational mode of the GaSe lattice, while the  $E_{2g}^1$  mode is associated with the in-plane

vibrational mode<sup>39</sup>. Then, the initial SHG signal of a GaSe-HCF is measured with bare HCF as a reference, where GaSe-HCF shows notably enhanced SHG at  $\sim 532 \text{ nm}$  and no obvious SHG signal from bare HCF at the low power density of excitation light with wavelength at  $\sim 1064 \text{ nm}$  (Fig. 2e). Moreover, under our optimized conditions, we have already realized long and uniform GaSe-HCF with lengths up to  $\sim 50 \text{ cm}$  (Fig. 2f). Obviously, with the proposed filling method, a great variety of nano-functional materials could be selectively filled into optical fibers with different porous structures, which could widely expand the applications in all-fiber functional devices. Herein, considering the loss-related effects and SHG transmission efficiency, a shorter fiber of 3–5 cm length is used in this paper.

For further exploring the SHG effect of GaSe-HCF, a home-built experimental optical system is employed (Fig. 3a,b). As a rule, an efficient nonlinear wavelength conversion process in an optical fiber happens under the condition that photon energy is within the bandgap of nonlinear material to avoid absorption. In this regard, a long wavelength of fundamental frequency (FW) light at  $\sim 1360 \text{ nm}$  (or  $\sim 0.91 \text{ eV}$ ) is chosen to generate SHG light at  $\sim 680 \text{ nm}$  (or  $\sim 1.82 \text{ eV}$ ), since the GaSe flakes have a direct bandgap of  $\sim 2.0 \text{ eV}$ <sup>40</sup>, where the energies of the incident and generated photons are both smaller than the bandgap to ensure low propagation loss at both excited and emitted wavelengths. To preliminarily test the transmission spectra of the GaSe-HCF, the spectra of the FW light and the SHG light are recorded (Fig. 3c,d) by the test system of transmission light as designed in Fig. 3b. The excitation laser (*i.e.*, FW light) at 1360 nm is focused on the fiber core by a  $\times 4$  microscope objective, and its polarization direction is varied by a half-wave plate (HWP) after a polarizer. The output SHG light beam from the GaSe-HCF (or bare HCF)

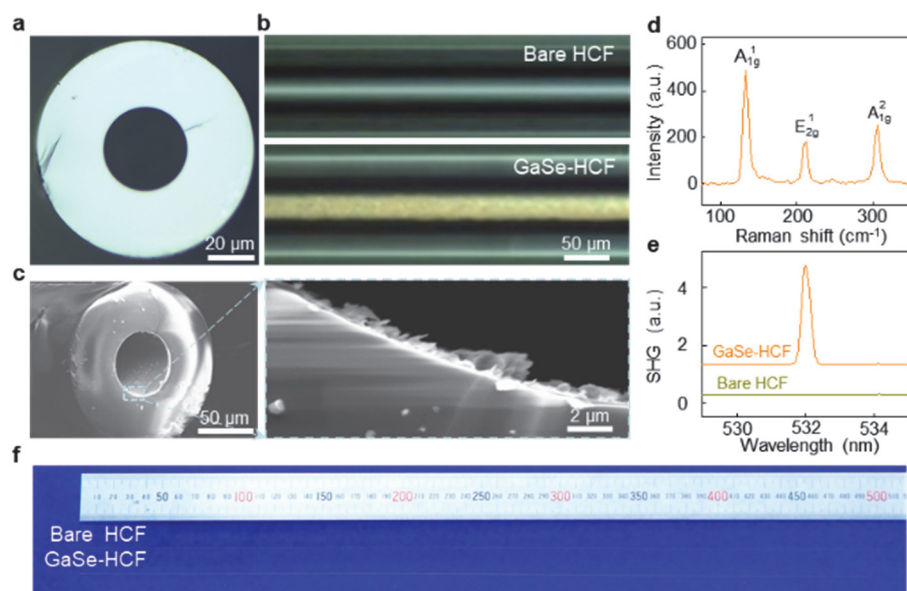
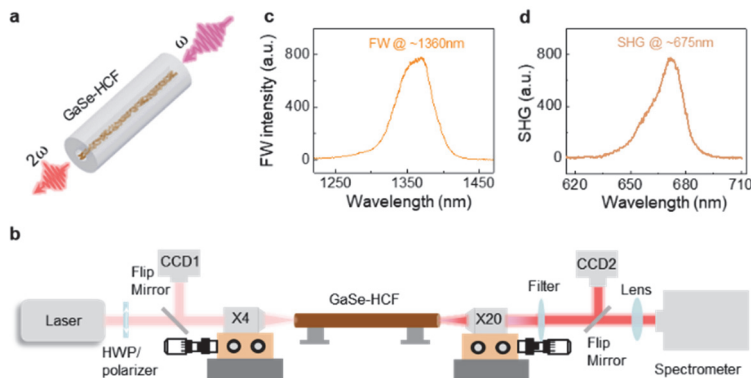


Fig. 2 Characteristic of GaSe-HCF.

(a) Optical image of the HCF with a core diameter of  $\sim 50 \mu\text{m}$ . (b) The corresponding side views of bare HCF and GaSe-HCF. (c) SEM image of a cross-section of GaSe-HCF.

(d) Raman spectrum of GaSe at the inner hole wall of the GaSe-HCF. (e) The spectra of the SHG for GaSe-HCF and bare HCF at the same excitation conditions.

(f) The GaSe-HCF with GaSe nanoflakes coated onto the inner hole walls with a length of up to half a meter.



**Fig. 3 Schematic of the experimental setup for SHG measurement and the initial optical transmission spectra.**

(a) Schematics of SHG ( $2\omega$ ) and FW ( $\omega$ ) in GaSe-HCF. (b) Schematic of the experimental setup for SHG measurements.

(c) The spectrum of the FW for an averaged input power. (d) The spectrum of the SHG emitted from the end of the GaSe-HCF.

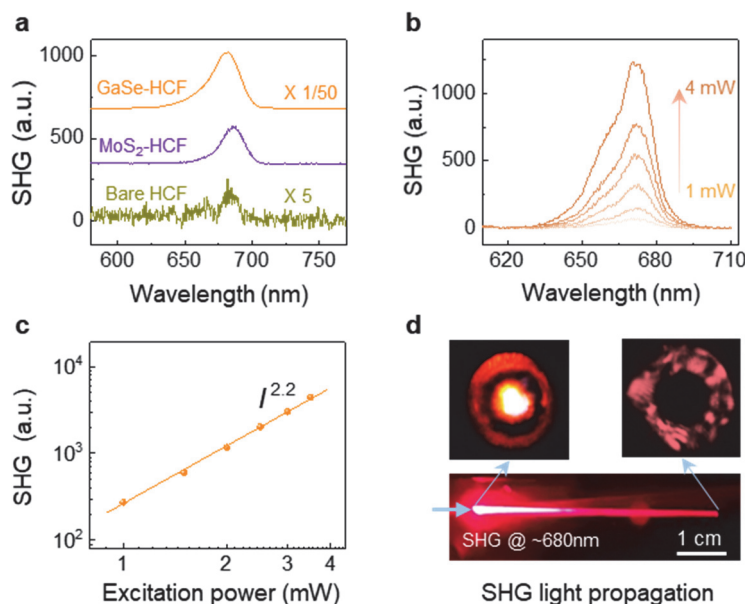


**Fig. 4 Greatly enhanced SHG in a few-centimeter GaSe-HCF and the SHG transmission properties.**

(a) The SHG spectra of GaSe-HCF, MoS<sub>2</sub>-HCF, and bare HCF under 1360 nm excitation. (b) The SHG spectra of GaSe-HCF with different input powers.

(c) Log-log plot between SHG power and input power of FW light for the GaSe-HCF. (d) The image of the SHG signal propagation in a GaSe-HCF.

is collected by a  $\times 20$  microscope object and imported into CCD and spectrometer after filtering the FW light by a filter. Two CCDs (labeled as CCD 1 and CCD 2) are placed respectively in the optical paths on both sides of the fiber, to record the transmission or reflection of the optical image from the two end surfaces of the fiber.

GaSe-HCF shows a much stronger enhanced SHG effect than MoS<sub>2</sub>-HCF, although two-dimensional MoS<sub>2</sub> is famous nonlinear material with an obvious SHG effect in the field of two-dimensional materials (Fig. 4a). Under the same condition, the SHG intensity from GaSe-HCF is nearly two orders of magnitude higher than that of MoS<sub>2</sub>-HCF, as shown in Fig. 4a. For ease of presentation, the SHG intensity from bare HCF has been scaled up by a factor of 5 and scaled down by a factor of 50 in GaSe-HCF (Fig. 4a). Here, the MoS<sub>2</sub>-HCF is fabricated by the chemical vapor deposition method as same as reported previously<sup>13</sup>. As a comparison, a bare HCF still shows a weak

SHG effect that originates from the inner surface between the air and silica of the HCF. This surface effect eventually leads to slight SHG due to centrosymmetry breaking at the surface<sup>14</sup>. These data indicate that the GaSe-HCFs are sufficiently available for some applications such as all-fiber optical frequency converters<sup>39</sup>. The SHG light increases exponentially with FW light with an index of ~2.2, which further confirms its second-order nonlinear process (Fig. 4b,c).

It is crucial for an efficient nonlinear process arising from direct interaction between the guided modes and materials, and thus the transmission process of SHG is recorded, as shown in Fig. 4d. The FW light at ~1360 nm is transmitted in the annular fiber core along a GaSe-HCF or a bare HCF. The FW light interacts with the GaSe-coating film through the evanescent light at the interface between the GaSe film and silica. The upper left panel in Fig. 4d is recorded by CCD 1 in Fig. 3b displays that most of the SHG signal (in red color) is generated in the hollow

core at the front end, but leaks into the air outside the fiber quickly when it propagates along the fiber with  $\sim 5$  cm length. This proves that the propagation mode is not a fundamental mode but a leak mode for the SHG at  $\sim 680$  nm. Meanwhile, the SHG signal can steadily propagate in the annular fiber core along the whole fiber, as in the upper right panel and bottom panel in Fig. 4d.

## 4 Conclusions

In summary, we proposed a novel syringe-filling method available for integrating HCF and nanomaterials where nanoflakes are coated on the fiber hole walls with fiber lengths up to half a meter. Based on this method, an all-fiber second harmonic frequency converter consisting of a GaSe-HCF demonstrates its strong light-matter interaction and a highly efficient SHG effect. The strong enhancement of SHG in GaSe-HCF is 2–3 orders of magnitude higher than that in MoS<sub>2</sub>-HCF or bare HCF. Our results may have an inspiration on the design and preparation of all-optical devices based on nano-functional materials, showing promise to expand the applications of nanomaterials in all-fiber systems.

## References

- (1) Fujii, Y.; Kawasaki, B. S.; Hill, K. O.; Johnson, D. C. *Opt. Lett.* **1980**, *5*, 48. doi: 10.1364/OL.5.000048
- (2) Canagasabey, A.; Corbari, C.; Gladyshev, A. V.; Liegeois, F.; Guillemet, S.; Hernandez, Y.; Yashkov, M. V.; Kosolapov, A.; Dianov, E. M.; Ibsen, M. *Opt. Lett.* **2009**, *34*, 16. doi: 10.1364/OL.34.002483
- (3) Pruneri, V.; Samoggia, F.; Bonfrate, G.; Kazansky, P. G.; Yang, G. *Appl. Phys. Lett.* **1999**, *74*, 17. doi: 10.1063/1.123868
- (4) Peter, G. K.; Philip, R.; Hiltromichi, T. *J. Lightwave Technol.* **1997**, *15*, 8. doi: 10.1109/50.618381
- (5) Ménard, J. M.; Russell, P. S. T. *Opt. Lett.* **2015**, *40*, 15. doi: 10.1364/OL.40.003679
- (6) Ménard, J. M.; Köttig, F.; Russell, P. S. T. *Opt. Lett.* **2016**, *41*, 16. doi: 10.1364/ol.41.003795
- (7) Feng, T. L.; Raabe, N.; Rustige, P.; Steinmeyer, G. *Appl. Phys. Lett.* **2018**, *112*, 24. doi: 10.1063/1.5030171
- (8) Kashyap, R. *Appl. Phys. Lett.* **1991**, *58*, 12. doi: 10.1063/1.104372
- (9) Myers, R. A.; Mukherjee, N.; Brueck, S. R. J. *Opt. Lett.* **1991**, *16*, 22. doi: 10.1364/OL.16.001732
- (10) Corbari, C.; Kazansky, P. G.; Slattery, S. A.; Nikogosyan, D. N. *Appl. Phys. Lett.* **2005**, *86*, 071106. doi: 10.1063/1.1868075
- (11) Canagasabey, A.; Corbari, C.; Zhang, Z. W.; Kazansky, P. G.; Ibsen, M. *Opt. Lett.* **2007**, *32*, 13. doi: 10.1364/OL.32.001863
- (12) Zhou, X.; Cheng, J. X.; Zhou, Y. B.; Cao, T.; Hong, H.; Liao, Z. M.; Wu, S. W.; Peng, H. L.; Liu, K. H.; Yu, D. P. *J. Am. Chem. Soc.* **2015**, *137*, 25. doi: 10.1021/jacs.5b04305
- (13) Zuo, Y. G.; Yu, W. T.; Liu, C.; Cheng, X.; Qiao, R. X.; Liang, J.; Zhou, X.; Wang, J. H.; Wu, M. H.; Zhao, Y. *Nat. Nanotechnol.* **2020**, *15*, 987. doi: 10.1038/s41565-020-0770-x
- (14) Jiang, B. Q.; Hao, Z.; Ji, Y. F.; Hou, Y. G.; Yi, R. X.; Mao, D.; Gan, X. T.; Zhao, J. L. *Light Sci. Appl.* **2020**, *9*, 63. doi: 10.1038/s41377-020-0304-1
- (15) Tong, L. M.; Lou, J. Y.; Mazur, E. *Opt. Express* **2004**, *12*, 6. doi: 10.1364/OPEX.12.001025
- (16) Schartner, E. P.; Dowler, A.; Ebendorf-Heidepriem, H. *Opt. Mater. Express* **2017**, *7*, 5. doi: 10.1364/OME.7.001496
- (17) Mo, J.; Feng, G. Z.; Liao, Y.; Yang, M.; Zhou, S. *High Power Laser Part. Beams* **2018**, *30*, 8. doi: 10.11884/HPLPB201830.180079
- (18) Dong, Q.; Liu, H. J. *J. Vib. Acoust.* **2019**, *141*, 3. doi: 10.1121/1.5101732
- (19) Yao, B. C.; Wu, Y.; Cheng, Y.; Zhang, A. Q.; Gong, Y.; Rao, Y. J.; Wang, Z. G.; Chen, Y. F. *Sensor Actuat. B-Chem.* **2014**, *194*, 142. doi: 10.1016/j.snb.2013.12.085
- (20) Shang, N. Z.; Cheng, Y.; Ao, S.; Tuerdi, G.; Li, M. W.; Wang, X. Y.; Hong, H.; Li, Z. H.; Zhang, X. Y.; Fu, W. Y.; et al. *Acta Phys. -Chim. Sin.* **2022**, *38*, 2108041. [尚念泽, 程熠, 敖申, 姑力米热, 李梦文, 王晓愚, 洪浩, 李泽晖, 张晓艳, 符汪洋, 等. 物理化学学报, 2022, 38, 2108041.] doi: 10.3866/PKU.WHXB202108041
- (21) Wei, W.; Nong, J. P.; Zhu, Y.; Zhang, G. W.; Wang, N.; Luo, S. Q.; Chen, N.; Lan, G. L.; Chuang, C. J.; Huang, Y. *Plasmonics* **2017**, *13*, 483. doi: 10.1007/s11468-017-0534-0
- (22) Huang, M.; Yang, C. H.; Sun, B.; Zhang, Z. X.; Zhang, L. *Opt. Express* **2018**, *26*, 3. doi: 10.1364/oe.26.0003098
- (23) Xin, W.; Liu, Z. B.; Sheng, Q. W.; Feng, M.; Huang, L. G.; Wang, P.; Jiang, W. S.; Xing, F.; Liu, Y. G.; Tian, J. G. *Opt. Express* **2014**, *22*, 9. doi: 10.1364/OE.22.010239
- (24) Corbari, C.; Gladyshev, A. V.; Lago, L.; Ibsen, M.; Hernandez, Y.; Kazansky, P. G. *Opt. Lett.* **2014**, *39*, 22. doi: 10.1364/ol.39.006505
- (25) Yu, Y.; Chen, H.; Zhang, Z. F.; Chen, D. B.; Yan, P. G. *Sensors* **2020**, *20*, 6. doi: 10.3390/s20061645
- (26) Li, W.; Chen, B. G.; Meng, C. Fang, W.; Xiao, Y.; Li, X. Y.; Hu, Z. F.; Fu, Y. X.; Tong, L. M.; Wang, H. Q.; et al. *Nano Lett.* **2014**, *14*, 2. doi: 10.1021/nl404356t
- (27) Gao, C.; Gao, L.; Zhu, T.; Yin, G. L. *Opt. Lett.* **2017**, *42*, 9. doi: 10.1364/OL.42.001708
- (28) Wang, R. D.; Li, D.; Jiang, M.; Wu, H.; Xu, X.; Ren, Z. Y. *Opt. Commun.* **2018**, *410*, 604. doi: 10.1016/j.optcom.2017.10.078
- (29) Wang, X. Y.; Fu, G. W.; Cui, Y. Z.; Fu, X. H.; Jin, W.; Bi, W. H. *App. Phys. Express* **2020**, *13*, 10. doi: 10.35848/1882-0786/abb95a
- (30) Bi, W. H.; Wang, Y. Y.; Fu, G. W.; Wang, X. Y.; Li, C. L. *Acta Phys. Sin.* **2016**, *65*, 4. [毕卫红, 王圆圆, 付广伟, 王晓愚, 李彩丽. 物理学报, 2016, 65, 4.] doi: 10.7498/aps.65.047801

- (31) Chen, K.; Zhou, X.; Cheng, X.; Qiao, R. X.; Cheng, Y.; Liu, C.; Xie, Y. D.; Yu, W. T. Yao, F. R.; Sun, Z. P.; *et al.* *Nat. Photonics* **2019**, *13*, 11. doi: 10.1038/s41566-019-0492-5
- (32) Guo, J.; Xie, J. J.; Li, D. J.; Yang, G. L.; Chen, F.; Wang, C. R.; Zhang, L. M.; Andreev, Y. M.; Kokh, K. A.; Lanskii, G. V.; *et al.* *Light Sci. Appl.* **2015**, *4*, e362. doi: 10.1038/lsci.2015.135
- (33) Cotter, D.; Manning, R. J.; Blow, K. J.; Ellis, A. D.; Kelly, A. E.; Nasset, D.; Phillips, I. D.; Poustie, A. J.; Rogers, D. C. *Science* **1999**, *286*, 5444. doi: 10.1126/science.286.5444.1523
- (34) Dudley, J. M.; Taylor, J. R. *Nat. Photonics* **2009**, *3*, 85. doi: 10.1038/nphoton.2008.285
- (35) Autere, A.; Jussila, H.; Dai, Y. Y.; Wang, Y. D.; Lipsanen, H.; Sun, Z. P. *Adv. Mater.* **2018**, *30*, 24. doi: 0.1002/adma.201705963
- (36) Li, Y.; Yi, R.; Mak, K. F.; You, Y.; Heinz, T. F. *Nano Lett.* **2013**, *13*, 7. doi: 10.1021/nl401561r
- (37) Tombelaine, V.; Buy-Lesvigne, C.; Leproux, P.; Couderc, V.; Melin, G. *Opt. Lett.* **2008**, *33*, 17. doi: 10.1364/OL.33.0002011
- (38) Segura, A.; Bouvier, J.; Andres M. V.; Manjon, F. J.; Munoz, V.; Bouvier, J. *Phys. Rev. B* **1997**, *56*, 7. doi: 10.1103/PhysRevB.56.4075
- (39) Allakhverdiev, K. R.; Yetis, M. O.; Baykara, T. K.; Salaev, E. Y. *Laser Phys.* **2009**, *19*, 5. doi: 10.1134/S1054660X09050375
- (40) Lei, S. D.; Ge, L. H.; Liu, Z.; Najmaei, S.; Shi, G.; You, G.; Lou, J.; Vajtai, R.; Ajayan, P. M. *Nano Lett.* **2013**, *13*, 2777. doi: 10.1021/nl4010089
- (41) Zhou, Y. B.; Nie, Y. F.; Liu, Y. J.; Yan, K.; Hong, J. H.; Jin, C. H.; Zhou, X.; Yin, J. B.; Liu, Z. F.; Peng, H. L. *ACS Nano* **2014**, *8*, 2. doi: 10.1021/nn405529r
- (42) Late, D. J.; Liu, B.; Matte, H. S. S; Rao, C. N. R.; Dravid, V. P. *Adv. Funct. Mater.* **2012**, *22*, 9. doi: 10.1002/adfm.201102913